How to Cite
Kabengele, C. N., Kasiama, G. N., Inkoto, C. L., Tshibangu, D. S.-T., Ngbolua, K.-T.-N., Mpiana, P. T., & Tshilanda, D. D. (2026). Electronic structure and visible-light response of a phosphonate-coordinated tungsten oxide (WO3) model: A first-principles study. *International Journal of Chemical & Material Sciences*, *9*(1), 1-9. https://doi.org/10.21744/ijcms.v9n1.2470

Electronic Structure and Visible-Light Response of a Phosphonate-Coordinated Tungsten Oxide (WO3) Model: A First-Principles Study

Carlos N. Kabengele
Department of Chemistry and Industry, Faculty of Science and Technology, University of Kinshasa, Democratic Republic of Congo
Corresponding author email: carlokabengele1@gmail.com

Giresse N. Kasiama
Department of Chemistry and Industry, Faculty of Science and Technology, University of Kinshasa, Democratic Republic of Congo
Email: giressekasiama@gmail.com

Clément L. Inkoto
E-PHYMED Laboratory, Department of Biology, Faculty of Science and Technology, BP 190 Kinshasa XI, University of Kinshasa, Democratic Republic of Congo
Email: clementinkoto@gmail.com

Damien S-T. Tshibangu
Department of Chemistry and Industry, Faculty of Science and Technology, University of Kinshasa, Democratic Republic of Congo
Email: tshibangud@gmail.com

Koto-Te-Nyiwa Ngbolua
E-PHYMED Laboratory, Department of Biology, Faculty of Science and Technology, BP 190 Kinshasa XI, University of Kinshasa, Democratic Republic of Congo
Email: jpngbolua@unikin.ac.cd

Pius T. Mpiana
Department of Chemistry and Industry, Faculty of Science and Technology, University of Kinshasa, Democratic Republic of Congo
Email: ptmpiana@gmail.com

Dorothée D. Tshilanda
Department of Chemistry and Industry, Faculty of Science and Technology, University of Kinshasa, Democratic Republic of Congo
Email: dtshilanda@gmail.com

Abstract---*The rational design of visible-light-active photocatalysts requires a detailed understanding of how local coordination environments modulate the electronic structure and key photocatalytic descriptors. In this work, we present a first-principles investigation of the electronic structure and optical properties of a tungsten–phosphonate metal–organic framework model using density functional theory. A minimal W–phosphonate cluster, consisting of a*

ISSN 2632-9468
Submitted: 27 January 2026 |Revised: 18 March 2026 | Accepted: 09 April 2026

WO_3 unit coordinated by phosphonate groups, is adopted to capture the essential features of the W–O–P motif while maintaining computational tractability. Electronic structure calculations performed at the PBE level reveal a semiconducting character with a valence band dominated by ligand-derived O 2p states and a conduction band primarily composed of W 5d orbitals, indicative of ligand-to-metal charge transfer (LMCT) excitations. Hybrid HSE06 calculations yield an improved band gap of 1.92 eV and enable an accurate alignment of band edges with respect to the vacuum level and water redox potentials. The resulting band positions indicate a strong thermodynamic driving force for the hydrogen evolution reaction, while oxygen evolution is found to be marginally accessible. Time-dependent DFT calculations further demonstrate pronounced visible-light absorption, with an intense band centered at approximately 545 nm originating from LMCT transitions. Overall, this study elucidates the electronic and optical consequences of phosphonate coordination on tungsten-based frameworks and provides atomistic insights relevant for the rational design of visible-light-responsive photocatalysts.
Keywords---*Tungsten phosphonate, Electronic structure, Visible-light photocatalysis, Density functional theory.*

Introduction

The development of photocatalytic materials capable of efficiently harvesting visible light represents a major challenge for applications such as environmental remediation and the conversion of solar energy into chemical fuels. To exhibit significant photocatalytic activity under solar irradiation, a material must simultaneously combine sufficient absorption in the visible region, efficient separation of photogenerated charge carriers, and band edge positions that are thermodynamically compatible with the targeted redox half-reactions (Abey et al., 2025). In practice, meeting these requirements concurrently remains difficult, which has motivated the rational design of advanced semiconductor systems through strategies such as band-gap engineering, heterostructure construction, and controlled defect modulation to enhance photocatalytic performance (Liu et al., 2025). Among the various strategies explored, tungsten-based materials, particularly tungsten trioxide (WO_3), have attracted considerable attention owing to their high chemical stability, suitable semiconducting properties, and strong oxidative capability under illumination. However, the photocatalytic performance of WO_3 remains intrinsically limited by several factors, including incomplete absorption of the solar spectrum, rapid recombination of photogenerated charge carriers, and band edge positions that are not always optimally aligned with the redox potentials of water, thereby restricting its overall photocatalytic efficiency (Linghua et al., 2025; He et al., 2026; Zhang et al., 2024; Quan et al., 2020). A promising strategy to overcome these limitations consists of tailoring the local coordination environment of tungsten centers through strongly coordinating ligands. Phosphonate groups are particularly attractive in this regard due to their high affinity for high-valent metal centers, their rich coordination versatility, and their ability to stabilize hybrid metal–oxygen architectures. Accordingly, phosphonate-based metal–organic frameworks and hybrid systems have demonstrated enhanced structural stability and tunable electronic structures, offering attractive opportunities for photocatalytic applications. Nevertheless, despite these advances, a detailed atomic-scale understanding of how phosphonate coordination modulates the local electronic structure and key photocatalytic descriptors of tungsten-based systems remains limited (Zhu et al., 2020; Zeng et al., 2020; Zhu et al., 2020). In this context, density functional theory (DFT) calculations provide a powerful framework to establish direct correlations between local coordination environments and the resulting electronic and optical properties. Semi-local generalized gradient approximation (GGA) functionals, such as the Perdew–Burke–Ernzerhof (PBE) functional, are widely employed to analyze the orbital composition of valence and conduction states as well as charge redistribution in hybrid systems. However, it is well recognized that PBE systematically underestimates electronic band gaps, which may affect the quantitative description of optical and photocatalytic properties. Hybrid functionals, such as HSE06, partially overcome this limitation by incorporating a fraction of exact exchange, leading to a more reliable description of the electronic band gap and band edge alignment, two critical descriptors for photocatalytic activity (Perdew et al., 1996; Heyd et al., 2003; Odoh et al., 2015; Henderson et al., 2011). In this work, we present a first-principles investigation of the electronic structure and visible-light photocatalytic properties of a tungsten phosphonate metal–organic framework model. A minimal structural model, consisting of a WO_3 unit coordinated by two phosphonate groups, is adopted to capture the local electronic features of the W–O–P motif while maintaining a reasonable computational cost. The electronic structure is first analyzed at the PBE level through total and projected density of states, frontier electronic states, and charge distribution analysis. Hybrid HSE06 calculations are subsequently performed to obtain a reliable electronic band gap and an accurate alignment of band edges with respect to the vacuum level and the redox potentials of water. Finally, the optical properties are evaluated to assess the visible-light absorption behavior. Altogether, these results elucidate how phosphonate coordination modulates the local electronic structure and

photocatalytic descriptors of tungsten-based hybrid systems, providing atomistic insights that are directly relevant for the rational design of visible-light-active photocatalysts.

Computational Details

Structural Model and Geometry Optimization

All first-principles calculations were performed within the framework of density functional theory (DFT). The initial structural model of the tungsten phosphonate system was constructed using the Avogadro molecular editor. To describe the system as an isolated cluster and avoid spurious interactions between periodic images, the model was placed in a cubic simulation cell with a lattice parameter of 20 Å, providing a sufficiently large vacuum region in all directions. Periodic boundary conditions were retained, while the large cell size ensured negligible mirror-image interactions. Structural relaxations were carried out until the residual forces on all atoms were below 10^{-3} Ry/Bohr.

Electronic Structure Calculations

Electronic structure calculations were performed using the Quantum ESPRESSO package. The interaction between valence electrons and ionic cores was described using norm-conserving ONCV pseudopotentials. Geometry optimizations and initial electronic structure calculations were carried out using the Perdew–Burke–Ernzerhof (PBE) exchange–correlation functional within the generalized gradient approximation (GGA). A kinetic energy cutoff of 120 Ry was employed for the plane-wave basis set. Brillouin zone sampling was restricted to the Γ point only, which is fully justified by the use of a large cubic supercell to model the system as an isolated cluster.

Density of States and Electronic Analysis

The electronic density of states (DOS) and projected density of states (PDOS) were obtained from non-self-consistent field calculations using an increased number of unoccupied bands to ensure a proper description of conduction states. Frontier electronic states and charge density distributions were visualized using VESTA.

Hybrid Functional Calculations and Band Edge Alignment

To obtain a more reliable description of the electronic band gap and band edge positions, additional calculations were performed using the HSE06 hybrid exchange–correlation functional, which incorporates a screened fraction of exact Hartree–Fock exchange. This approach partially corrects the systematic underestimation of band gaps inherent to semi-local GGA functionals and provides an improved description of the electronic structure relevant for photocatalytic applications (Islam, 2024). The alignment of the valence band maximum (VBM) and conduction band minimum (CBM) with respect to the vacuum level was determined using the electrostatic potential reference. The planar-averaged electrostatic potential was evaluated in the vacuum region of the supercell, allowing the band edge positions to be placed on an absolute energy scale and directly compared with the redox potentials of water.

Optical Properties Calculations

Because the W–phosphonate framework is modeled as an isolated cluster embedded in a large periodic cell, its optical response is more appropriately described using a molecular excited-state approach. Therefore, TD-DFT calculations were performed (ORCA) to obtain the UV–Vis spectrum and to assign the dominant transitions, which are consistent with the LMCT character inferred from the PBE PDOS and frontier-state analysis.

Results

Structural Model and Local Coordination Environment

Figure 1 below shows the optimized structural model of the relaxed W-phosphonate cluster, highlighting the local W–O–P coordination environment.

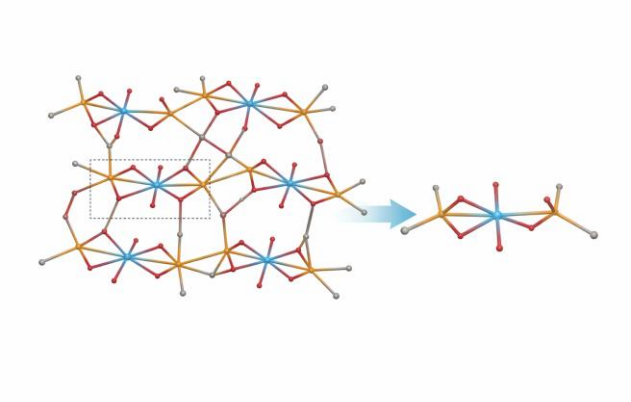

Figure 1. Optimized geometry of the W-phosphonate system

The optimized geometry reveals two phosphonate oxygen atoms bridging the tungsten center, giving rise to well-defined W–O–P linkages. The corresponding W–O bond lengths (2.033 and 2.066 Å) are significantly longer than the terminal W=O distances, consistent with a bridging coordination mode. The associated P–O distances (1.573 – 1.590 Å) further indicate the involvement of phosphonate oxygen atoms in metal coordination. The W–O–P angles of 102.35° and 104.16° fall within the typical range reported for phosphonate-bridged metal centers, confirming a stable local coordination environment (Clearfield & Demadis, 2011).

Electronic Structure at the PBE Level
Total and Projected Density of States (DOS/PDOS)

The total density of states (DOS) and the projected density of states (PDOS) were calculated based on the optimized geometry at the PBE level; results are presented in Figure 2 below. The Fermi level is set to 0 eV and indicated by the dashed vertical line.

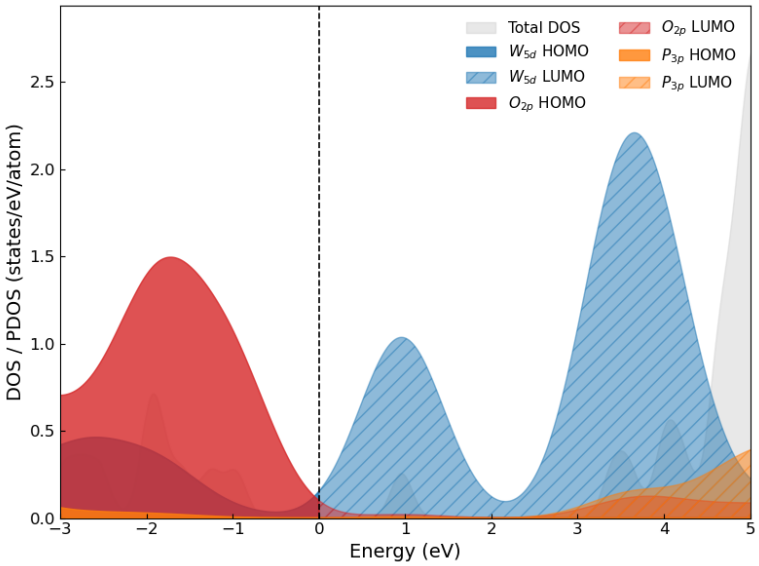

Figure 2. PBE-Calculated Total and Projected Density of States

The system exhibits a clear semiconducting character. The valence band maximum (VBM) is primarily composed of O 2p states, with a minor contribution from P 3p orbitals, indicating that the valence-edge electronic structure is dominated by ligand-derived states. In contrast, the conduction band minimum (CBM) is largely governed by W 5d orbitals, revealing the metal-centered nature of the low-lying unoccupied states. This orbital distribution establishes the electronic origin of the band edges and points to a ligand-to-metal-dominated excitation across the band gap.

Frontier Electronic States and Charge Distribution

To gain insight into the nature of the frontier electronic states, the spatial distributions of the HOMO- and LUMO-like band-edge states of the W–phosphonate framework were analyzed at the PBE level as shown in Figure 3. The HOMO is mainly localized on the phosphonate oxygen atoms and adjacent carbon moieties, indicating a ligand-centered character of the valence-edge states. In contrast, the LUMO is predominantly distributed over the tungsten center, with a strong contribution from W 5d orbitals, revealing a metal-centered nature of the conduction-edge states.

Figure 3. Frontier molecular orbitals of the W–phosphonate framework calculated at the PBE level: (a) HOMO and (b) LUMO isosurfaces plotted at an isovalue of 0.003 e Å^{-3}. Positive and negative phases of the wavefunction are represented in red and blue, respectively

This clear spatial separation between the highest occupied and lowest unoccupied states is characteristic of a ligand-to-metal charge transfer (LMCT) excitation, which is widely recognized as beneficial for photocatalytic activity by promoting charge separation and suppressing electron–hole recombination (Kudo & Miseki, 2008), Such an electronic configuration is consistent with that reported for other d^0 transition-metal phosphonate- and oxo-based frameworks, where ligand-derived O 2p states dominate the valence band edge, while metal d states define the conduction band edge (Pacchioni, 2003; Di Valentin et al., 2013; Li et al., 2024). To further support this interpretation, a Löwdin population analysis was performed to quantify the charge distribution within the framework, and results are presented in Table 1.

Table 1
Löwdin Atomic Charges Calculated at the PBE Level

Element	Zval	NLöwdin (e)	Charge (e)
W	14	12.78	+1.22
P	5	3.18	+1.82
O	6	6.60	−0.60
C	4	4.70	−0.70
H	1	0.76	+0.24

Tungsten exhibits a positive partial charge of +1.22 e, while oxygen atoms carry significant negative charges (−0.60 e), reflecting strong W–O polarization. Phosphorus atoms are also positively charged (+1.82 e), consistent with electron donation toward the metal–oxygen framework. Although the absolute values of atomic charges depend on the population scheme employed, the pronounced metal–ligand polarization observed here is robust and in good agreement with previous theoretical studies on phosphonate-based metal–organic systems (Mancuso et al., 2020). Overall, the combined frontier orbital and charge analyses confirm an efficient electronic polarization within our system, which is expected to favor photoinduced charge separation and enhance photocatalytic redox processes.

Band Gap Correction and Band Edge Alignment (HSE06)

As expected for a semi-local GGA functional, the PBE band gap is underestimated, motivating the use of hybrid functionals for a more accurate description of the electronic structure (Rosen et al., 2022). Accordingly, the photocatalytic feasibility of the system was assessed using the HSE06 functional. The planar-averaged electrostatic potential was computed to define an absolute vacuum reference, enabling alignment of the HSE06 band edges with respect to the water redox potentials, as illustrated in Figure 4.

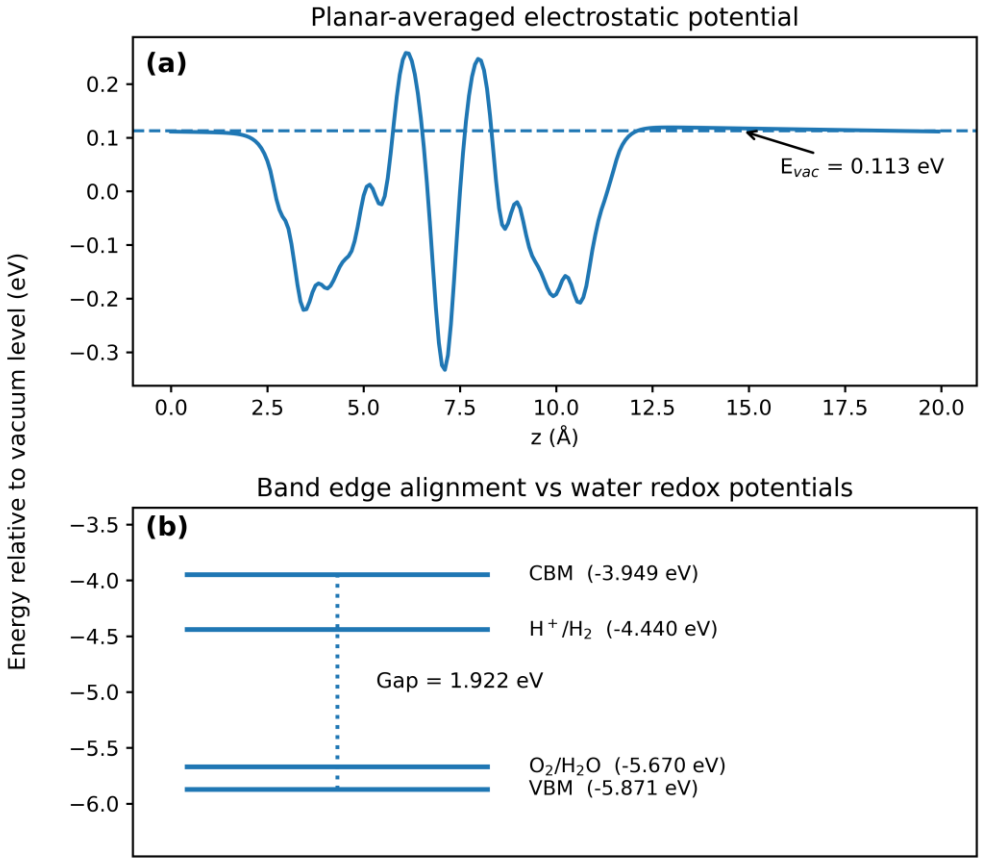

Figure 4. Band edge alignment relative to water redox potentials calculated at the HSE06 level. (a) Planar-averaged electrostatic potential along the z direction obtained from HSE06 calculations, showing the vacuum reference level extracted from the asymptotic region. (b) Absolute positions of the valence band maximum (VBM) and conduction band minimum (CBM) aligned to the vacuum level and compared with the redox potentials of H^+/H_2 and O_2/H_2O.

At the PBE level, a narrow band gap of 1.03 eV was obtained from the total density of states, which is consistent with the well-known tendency of semi-local GGA functionals to underestimate band gaps in metal–organic and oxide-based semiconductors. In contrast, the HSE06 hybrid functional yields a substantially widened band gap of 1.92 eV, providing a more reliable description of the electronic structure. Previous hybrid DFT studies on pristine (WO_3) have reported band gaps typically in the range of ~2.5–2.8 eV, depending on the crystal phase and computational methodology. These values are consistently higher than the band gap obtained for the present W–phosphonate model, indicating that ligand incorporation effectively narrows the band gap and induces a red shift in the optical response toward the visible region, enhancing photocatalytic performance (Zhu et al., 2020; Kerr et al., 2025; Zhu et al., 2019; Hajiahmadi & Azar, 2022). In a closely related study, Peeples et al. (2022), demonstrated that the electronic structure of phosphonate-based MOFs can be strongly modulated by the coordination environment of the metal nodes. In the Cu-phosphonate framework TUB1, the coexistence of square-planar and trigonal-bipyramidal Cu centers was shown to induce a significant reduction of the band gap. Optical measurements revealed visible-light band gaps of 2.4 eV (indirect) and 2.7 eV (direct), while DFT calculations highlighted a pronounced spin-dependent electronic structure. In particular, the lowest unoccupied states were found to be predominantly localized on the square-planar Cu sites, which effectively narrow the overall band gap compared to the trigonal-bipyramidal Cu environments. Nevertheless, more generally, previous studies on d^0 transition-metal-based MOFs and coordination frameworks have consistently shown that hybrid functional calculations yield band gaps in the visible range, commonly between ~1.8 and 2.5 eV, placing the present results well within the established literature trends. For

instance, in the phosphonate MOF TUB75 studied by Siemensmeyer et al. 2020), the experimental UV-Vis gap was ~1.4 eV, and the DFT-calculated band gap was 1.77 eV, aligning well with the band gap range observed in the present work. Similarly, Syzgantseva et al. (2019), demonstrated through hybrid HSE06 calculations that d^0 transition-metal–based MOFs exhibit band gaps typically ranging between ~1.8 and 2.4 eV depending on the metal node and linker chemistry, in good agreement with the HSE06 band gap reported here. The absolute band-edge positions derived from HSE06 calculations further support the photocatalytic potential of the W–phosphonate framework. The conduction band minimum (−3.95 eV) lies well above the H^+/H_2 reduction potential (−4.44 eV), indicating that photogenerated electrons possess sufficient reducing power to drive the hydrogen evolution reaction (HER). Meanwhile, the valence band maximum (−5.87 eV) is located slightly below the O_2/H_2O oxidation potential (−5.67 eV), suggesting that oxygen evolution is thermodynamically accessible but less favorable, in line with previous studies reporting HER-selective activity for phosphonate-based and metal–oxo hybrid frameworks. The band-gap correction and band-edge alignment at the HSE06 level place the W–phosphonate framework among a growing class of visible-light-active MOF-based photocatalysts, with a strong thermodynamic driving force for HER and a more marginal but potentially accessible OER pathway under suitable kinetic or surface catalytic conditions.

Optical Properties and Visible-Light Absorption

Figure 5 displays the TD-DFT calculated UV–vis absorption spectrum of the W–phosphonate model framework, evidencing a pronounced extension of light absorption into the visible region driven by ligand-to-metal charge transfer (LMCT) transitions.

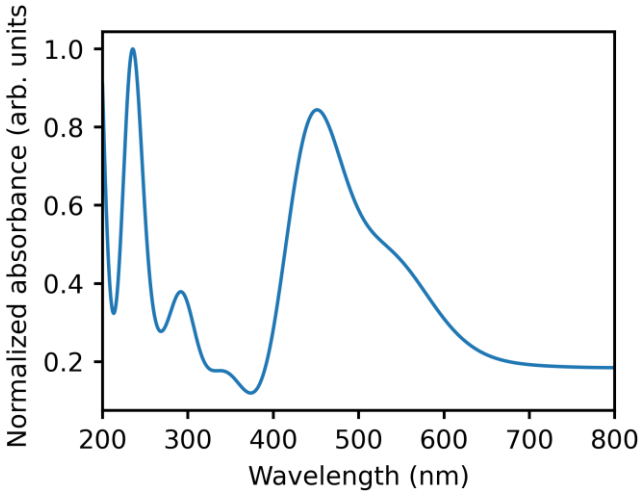

Figure 5. Calculated UV–vis absorption spectrum of the phosphonate-functionalized WO_3 cluster obtained from TD-DFT calculations

The calculated UV–vis absorption spectrum shows an absorption onset in the visible region, with a pronounced, intense band centered at approximately 545 nm (2.27 eV). This band corresponds to the most intense electronic transition in the visible range and is associated with a relatively high oscillator strength (f = 0.149). Similar visible-light absorption features have been reported for phosphonate-based metal–organic frameworks and tungsten-oxide hybrid systems, in which ligand coordination induces low-energy charge-transfer states within the pristine oxide framework's band gap [25,26]. A detailed TD-DFT excited-state analysis reveals that this visible absorption originates from a mixed electronic excitation dominated by transitions from several occupied orbitals into the lowest-lying acceptor states. In particular, STATE 12 is mainly composed of 73a → 80a (0.396) and 71a → 80a (0.282) contributions, with additional intensity arising from 75a → 81a (0.123) and 72a → 81a (0.077) transitions. The recurrent involvement of the same low-energy virtual orbitals (80a/81a) indicates that photoexcited electrons are preferentially funneled into WO_3-centered acceptor states. Such behavior is characteristic of ligand-to-metal charge transfer (LMCT) excitations commonly observed in d^0 transition-metal–based phosphonate frameworks and metal–oxo hybrid photocatalysts [9,22–24]. The recurrent involvement of the same low-energy virtual orbitals (80a/81a) indicates that photoexcited electrons are preferentially funneled into WO_3-centered acceptor states, which is consistent with a ligand-to-metal charge transfer (LMCT) character induced by phosphonate functionalization. In the ultraviolet region below 300 nm, several intense absorption features are observed. These high-energy bands can be

attributed to intrinsic oxide-centered and ligand-localized electronic excitations, in agreement with previous theoretical and experimental studies on WO_3 and related phosphonate-functionalized metal oxides (Di Valentin et al., 2013; Zhu et al., 2019). These optical assignments are fully consistent with the electronic structure analysis presented above. At the PBE level, the valence band maximum is predominantly composed of ligand-derived O 2p states with minor P 3p contributions, whereas the conduction band minimum is dominated by W 5d orbitals. This electronic configuration is widely recognized as a favorable condition for LMCT-driven optical absorption and photoinduced charge separation in phosphonate-based MOFs and tungsten-oxide photocatalysts (Syzgantseva et al., 2019; Peeples et al., 2022). The coexistence of strong ultraviolet absorption and a pronounced visible-light response highlights the dual-band optical behavior of the studied system. Similar dual UV–visible absorption characteristics have been identified in other phosphonate-based and tungsten-containing photocatalytic systems, where ligand-induced electronic coupling effectively extends light harvesting into the visible region while preserving strong UV activity (Islam, 2024; Di Valentin et al., 2013). This behavior supports the potential of the present W–phosphonate framework for visible-light-driven photocatalytic applications, particularly hydrogen evolution.

Conclusion

In summary, a comprehensive first-principles study has been carried out to elucidate the electronic structure and visible-light photocatalytic properties of a tungsten–phosphonate metal–organic framework model. Density of states and frontier-orbital analyses at the PBE level reveal a clear separation between ligand-centered valence states and tungsten-centered conduction states, establishing a ligand-to-metal charge transfer electronic configuration that is favorable for photoinduced charge separation. Hybrid HSE06 calculations provide a more reliable description of the band gap and band-edge positions, demonstrating that phosphonate coordination effectively narrows the band gap relative to pristine WO_3 and shifts the optical response into the visible region. The absolute band alignment indicates that photogenerated electrons possess sufficient reducing power to drive hydrogen evolution, while oxygen evolution remains thermodynamically less favorable. Time-dependent DFT calculations corroborate these findings by revealing intense visible-light absorption bands associated with LMCT transitions. Altogether, these results highlight the critical role of phosphonate ligands in tailoring the electronic structure and photocatalytic descriptors of tungsten-based hybrid systems. The insights obtained in this work offer a rational framework for the design of phosphonate-functionalized metal–oxo materials for visible-light-driven photocatalytic applications.

References

Abey, S. A., Reis, N. M., Emanuelsson, E. A., & Expósito, A. J. (2025). Harnessing visible light: Advanced photocatalytic strategies for sustainable environmental reactions. *Chemical Engineering Journal*, *519*, 164951. https://doi.org/10.1016/j.cej.2025.164951

Clearfield, A., & Demadis, K. (Eds.). (2011). *Metal phosphonate chemistry: From synthesis to applications*. Royal Society of Chemistry.

Di Valentin, C., Wang, F., & Pacchioni, G. (2013). Tungsten oxide in catalysis and photocatalysis: hints from DFT. *Topics in Catalysis*, *56*(15), 1404-1419.

Hajiahmadi, Z., & Azar, Y. T. (2022). Computational study of h-WO3 surfaces as a semiconductor in water-splitting application. *Surfaces and Interfaces*, *28*, 101695. https://doi.org/10.1016/j.surfin.2021.101695

He, L., Yu, C. B., Lu, K. Q., Yang, K., Huang, W. Y., & Li, D. (2026). Recent advances in synthesis, performance, and application of oxygen vacancy-enriched WO3− x photocatalysts. *Tungsten*, *8*(1), 8-36.

Henderson, T. M., Paier, J., & Scuseria, G. E. (2011). Accurate treatment of solids with the HSE screened hybrid. *physica status solidi (b)*, *248*(4), 767-774.

Heyd, J., Scuseria, G. E., & Ernzerhof, M. (2003). Hybrid functionals based on a screened Coulomb potential. *The Journal of chemical physics*, *118*(18), 8207-8215.

Islam, M. (2024). A comprehensive investigation on the physical properties of SiC polymorphs for high-temperature applications: A DFT study based on GGA and hybrid HSE06 exchange correlation functionals. *Nuclear Materials and Energy*, *38*, 101631. https://doi.org/10.1016/j.nme.2024.101631

Kerr, R. D., Gilbert, M. R., & Murphy, S. T. (2025). Relating the formation energies for oxygen vacancy defects to the structural properties of tungsten oxides. *Computational Materials Science*, *252*, 113781. https://doi.org/10.1016/j.commatsci.2025.113781

Kudo, A., & Miseki, Y. (2008). Heterogeneous photocatalyst materials for water splitting. *Chemical Society Reviews*, *38*(1), 253-278.

Li, X. S., He, Y. J., Chen, J., Li, Q. Q., Liu, P., & Li, J. L. (2024). Recent advances in rational design, synthesis and application of metal–organic frameworks as visible-light-driven photocatalysts. *Inorganic Chemistry Frontiers*, *11*(20), 6794-6852.

Linghua, B., Lingxiao, T., Zhang, S., Xu, K., & Chengchu, Z. (2025). Recent Progress in WO3-Based Photo (electro)-Catalysis Systems for Green Organic Synthesis and Wastewater Remediation: A Review. *Catalysts*, *15*(11), 1061.

Liu, J., Zhao, D., Wu, X., Wu, D., Su, N., Wang, Y., ... & Zhang, Q. (2025). Synergistic dual-defect band engineering for highly efficient photocatalytic degradation of microplastics via Nb-induced oxygen vacancies in SnO2 quantum dots. *Journal of Materials Chemistry A*, *13*(6), 4429-4443.

Mancuso, J. L., Mroz, A. M., Le, K. N., & Hendon, C. H. (2020). Electronic structure modeling of metal–organic frameworks. *Chemical reviews*, *120*(16), 8641-8715.

Odoh, S. O., Cramer, C. J., Truhlar, D. G., & Gagliardi, L. (2015). Quantum-chemical characterization of the properties and reactivities of metal–organic frameworks. *Chemical reviews*, *115*(12), 6051-6111.

Pacchioni, G. (2003). Oxygen vacancy: the invisible agent on oxide surfaces. *ChemPhysChem*, *4*(10), 1041-1047.

Peeples, C. A., Çetinkaya, A., Tholen, P., Schmitt, F. J., Zorlu, Y., Bin Yu, K., ... & Yücesan, G. (2022). Coordination-Induced Band Gap Reduction in a Metal–Organic Framework. *Chemistry–A European Journal*, *28*(8), e202104041.

Perdew, J. P., Burke, K., & Ernzerhof, M. (1996). Generalized gradient approximation made simple. *Physical review letters*, *77*(18), 3865.

Quan, H., Gao, Y., & Wang, W. (2020). Tungsten oxide-based visible light-driven photocatalysts: crystal and electronic structures and strategies for photocatalytic efficiency enhancement. *Inorganic Chemistry Frontiers*, *7*(4), 817-838.

Rosen, A. S., Fung, V., Huck, P., O'Donnell, C. T., Horton, M. K., Truhlar, D. G., ... & Snurr, R. Q. (2022). High-throughput predictions of metal–organic framework electronic properties: theoretical challenges, graph neural networks, and data exploration. *npj Computational Materials*, *8*(1), 112.

Siemensmeyer, K., Peeples, C. A., Tholen, P., Schmitt, F. J., Çoşut, B., Hanna, G., & Yücesan, G. (2020). Phosphonate metal–organic frameworks: A novel family of semiconductors. *Advanced Materials*, *32*(24), 2000474.

Syzgantseva, M. A., Ireland, C. P., Ebrahim, F. M., Smit, B., & Syzgantseva, O. A. (2019). Metal substitution as the method of modifying electronic structure of metal–organic frameworks. *Journal of the American Chemical Society*, *141*(15), 6271.

Zeng, T., Shi, D., Cheng, Q., Liao, G., Zhou, H., & Pan, Z. (2020). Construction of novel phosphonate-based MOF/P–TiO2 heterojunction photocatalysts: enhanced photocatalytic performance and mechanistic insight. *Environmental Science: Nano*, *7*(3), 861-879.

Zhang, F., Han, W., Cai, J., Shen, B., & Guo, S. Q. (2024). WO3· nH2O-based photocatalysts: structural analysis, rational design, and applications in energy conversion and environmental remediation. *Fuel*, *365*, 131289. https://doi.org/10.1016/j.fuel.2024.131289

Zhu, F., Ma, C., Gu, L., Chen, G., Zhang, J., Cong, S., ... & Zhang, X. (2019). Off-centered-symmetry-based band structure modulation of hexagonal WO3. *Journal of Physics: Condensed Matter*, *31*(35), 355501.

Zhu, Y. P., Yin, J., Abou-Hamad, E., Liu, X., Chen, W., Yao, T., ... & Alshareef, H. N. (2020). Highly stable phosphonate-based MOFs with engineered bandgaps for efficient photocatalytic hydrogen production. *Advanced Materials*, *32*(16), 1906368.

Zhu, Y. P., Yuan, Z. Y., & Alshareef, H. N. (2020). New opportunities for functional materials from metal phosphonates. *ACS Materials Letters*, *2*(6), 582-594.